dx.doi.org/10.14227/DT210214P31

Development of a Discriminative Intrinsic Dissolution Method for Efavirenz

e-mail: valeria@pharma.ufrj.br

Eduardo Costa Pinto, Lucio Mendes Cabral, and Valéria Pereira de Sousa*

Department of Pharmaceutics, Faculty of Pharmacy, Federal University of Rio de Janeiro, Av. Carlos Chagas Filho, 373, CCS, Bss, sala 15, Rio de Janeiro, RJ, 21941-902, Rio de Janeiro, Brazil

ABSTRACT

Efavirenz is a poorly water-soluble drug categorized as a Class 2 drug under the Biopharmaceutics Classification System (BCS). Intrinsic dissolution is an effective tool for evaluating the physical–chemical properties of an active pharmaceutical ingredient (API). The aim of this study was to develop an intrinsic dissolution method for use in quality control of efavirenz to be used in the selection of an API for the production of dosage forms. The influence of compression force, rotation speed, dissolution medium, and surfactant concentration on the intrinsic dissolution rate (IDR) of efavirenz were evaluated using a rotating-disk holder. The developed method was applied to the evaluation of batches using different raw materials (batches A–G). Dissolution media containing 0.5% sodium lauryl sulfate (SLS) and a rotation speed of 100 rpm proved the most discriminative. Batches A, D, and F provided intrinsic dissolution rate (IDR) values greater than 36 μg/min/cm^2 in this medium, while batches B and E provided IDR values of approximately 31 μg/min/cm^2. The IDRs obtained showed a high correlation with the surface areas of the batches. The method may be used in the development of efavirenz formulations to select API with physical–chemical properties that enable appropriate dosage form dissolution.

KEYWORDS: Efavirenz; intrinsic dissolution; rotating disc; Wood's apparatus; surface area; particle size distribution.

INTRODUCTION

Efavirenz is an antiviral drug used worldwide in the treatment of acquired immune deficiency syndrome (AIDS). It is the non-nucleoside inhibitor of the reverse transcriptase enzyme indicated by the World Health Organization for polytherapy against the human immunodeficiency virus (*1–3*). This drug is categorized as Class 2 (low solubility and high permeability) according to the Biopharmaceutics Classification System (BCS), thus its low solubility (pK_a = 10.2 and log P = 5.4) limits dissolution of its dosage forms (*4*, *5*). Alternative approaches to improve efavirenz dissolution were reported, such as the use of superdisintegrants (*6*), complexation with cyclodextrin (*7*, *8*), production of solid dispersions (*9*, *10*), and the use of nanotechnology for the preparation of polymeric micelles containing efavirenz (*11*, *12*). However, beyond issues with formulations, physical–chemical properties of the API including particle size distribution, specific surface area, polymorphism, and degree of hydration have direct impact on dosage form dissolution (*13–15*), and the use of low quality raw materials may result in formulations with bioavailability limitations (*16*, *17*).

Intrinsic dissolution is an official method for the evaluation of drug powders and has wide application in characterizing drugs during the formulation development. It is an effective tool for evaluating the physical–chemical properties of an API upon dissolution without the influence of excipients (*18*, *19*). Differences related to drug polymorphism and crystalline structure can be revealed by the IDR (*20–22*) and can be used for biopharmaceutical classification of drugs (*23–25*). A discriminative intrinsic dissolution method may indicate the differences that exist between API batches obtained from the same supplier as well as evaluate distinct suppliers of the same API. This would allow monitoring of the quality of raw materials and assist in batch selection of raw materials with physical–chemical properties that are appropriate for formulation development (*26–29*).

Although the intrinsic dissolution method is described in a *USP* general chapter, there are no official drug monographs available; therefore, test parameters such as disk compression force, rotation speed, and dissolution media have to be evaluated for each drug to establish an intrinsic dissolution method (*19*). Dissolution methods for tablets, capsules, and oral efavirenz solutions have been reported in the major pharmacopeias and by the FDA (*19*, *30–32*); however, until now there was no official method described for intrinsic dissolution evaluation of this drug. The purpose of this study was to develop an intrinsic dissolution method for the quality control of efavirenz raw materials to be used for API selection. In addition, the physical–chemical properties of the API will be evaluated, which will enable production of dosage forms with appropriate dissolution properties and bioavailability. This work also aimed to apply the developed method to the evaluation of different raw materials in efavirenz batches.

*Corresponding author.

MATERIALS AND METHODS

Chemicals and Reagents

The reagents ammonium acetate, monobasic potassium phosphate, polysorbate 80 (Tween 80), sodium chloride, sodium hydroxide, and sodium lauryl sulfate (SLS) were acquired from Vetec (Rio de Janeiro, Brazil). Chromatographic grade acetonitrile and methanol were purchased from Tedia (Rio de Janeiro, Brazil). All solutions were prepared using Milli-Q water (Millipore, Bedford, MA, USA). The 100.0% pure efavirenz standard was supplied by Globe Química (São Paulo, Brazil). Seven batches of raw materials (batches A–G) were acquired from three different Brazilian suppliers: Nortec Química (Rio de Janeiro, Brazil), Globe Química, and Cristália Produtos Químicos Farmacêuticos Ltda (São Paulo, Brazil). Batches A and B were used for the production of tablets by Farmanguinhos Laboratories (Rio de Janeiro, Brazil). Tablets obtained from batch A were bioequivalent to the reference drug Stocrin, while tablets prepared with batch B were not bioequivalent (*33*). Batches A003352 and A006610 of the reference medication Stocrin (Merck Sharp & Dohme, NJ, USA) were used in the bioequivalence studies of biobatches A and B, respectively. Biobatch B used in the bioequivalence study showed values of C_{max} and *AUC* that were 56% and 52% less than the reference, respectively, with the same T_{max} of 4.5 h (*33*).

Drug Characterization

X-ray Powder Diffraction

X-ray diffraction (XRD) was performed to verify drug polymorphism and crystalline structure. Powder samples were analyzed in an X-ray diffractometer (Higaku Miniflex, Tokyo, Japan) operated with a voltage of 30 kV, a current of 15 mA, a step size of 0.05°, a 1 °C/min scan speed, at room temperature and using CuK_2 radiation. Samples were scanned with an angular range between the 1° and 40° 2θ scale.

Differential Scanning Calorimetry

Differential scanning calorimetry (DSC) (Shimadzu, DSC-60, Columbia, MD, USA) was carried out by weighing 2-mg samples of the drug substance into an aluminum pan, which was scanned from 25 to 250 °C using a heating rate of 10 °C/min and a nitrogen gas flow rate of 50 mL/min.

Particle Size Analysis

The particle size distribution was measured by laser diffraction using the wet mode (Malvern Mastersizer 2000, Hydro 2000 SM; Worcestershire, UK). Samples were prepared using approximately 10 mg of the drug substance, which was dispersed in a beaker containing 10 mL of 0.02% (w/v) polysorbate 80 solution. The dispersion medium was 100 mL of water, and the rotation speed was 2000 rpm. Particle size analyses were evaluated considering the parameters of mean, median, mode, and polydispersion index (PI).

Specific Surface Area

The specific surface areas of the efavirenz batches were evaluated by nitrogen gas adsorption (Micromeritics Gemini VI 2385C, Norcross, GA, USA). Samples were degassed at 25 °C for 24 h under a vacuum that generated pressures of 500 mm Hg/min, and the equilibrium time for adsorption was 70 s. The amount of nitrogen gas adsorbed was calculated using the Brunauer, Emmett, and Teller (BET) method with a relative pressure range of ($0.05 < P/P_0 < 0.35$).

Scanning Electron Microscopy

The morphology of the raw materials was determined by scanning electron microscopy (SEM) (Jeol, JSM-5310, Tokyo, Japan). The samples were mounted with carbon adhesive onto an aluminum holder, and the surface was sputter-coated with gold for 2 min (Sputtering Balzers, FL 9496, Balzers, LI) and photographed at a voltage of 20 kV.

Solubility

The solubility of efavirenz was evaluated by adding an excess amount of sample into a beaker containing 10 mL of medium. The media used were 0.1 N hydrochloric acid pH 1.2, 0.05 M acetate buffer pH 4.5, water pH 5.5, and 0.05 M sodium phosphate buffer pH 6.8 (*19*). All media were evaluated without surfactant and at concentrations of 0.5, 1.0, and 2.0% (w/v) SLS. Samples were agitated using a magnetic stirrer at 50 rpm for 24 h at 25 °C. Subsequently, samples were centrifuged at 3500 rpm for 30 min and filtered through a 0.45-µm pore membrane, and the concentration was determined by UV-vis spectrophotometer (Vankel 50, Varian Inc., Palo Alto, CA, USA) using a wavelength of 248 nm. All experiments were analyzed in triplicate with the same batch of API (batch D) that was used for all solubility analyses.

Development of the Intrinsic Dissolution Method

The intrinsic dissolution method was developed using a rotating disk holder similar to the one proposed by Wood et al. (*34*) with a surface area of 0.5 cm^2. Disks of the efavirenz drug substance were prepared by compressing 180 mg of sample with a hydraulic press (QLA 2 Ton Universal Press, NJ, USA). Dissolution studies were performed at a temperature of 37 ± 0.5 °C in a Hanson Research SR6 dissolution tester (Hanson Research Corp., Chatsworth, CA, USA). The distance between the intrinsic die and the bottom of the vessel was 3.8 cm. Aliquots of 5 mL were withdrawn using a 10-µm cannula filter at 15, 30, 45, 60, 90, 120, 150, 180, 210, 240, 270, and 300 min. The concentration of efavirenz in the solution was measured by UV spectrophotometer at a wavelength of 248 nm (Vankel 50, Varian Inc., Palo Alto, CA, USA) according to the drug monograph (*19*). Sink conditions were maintained during the experiment. All measurements were performed in triplicate. Subsequently, batch D was used during the development of the intrinsic dissolution method.

The parameters of disk compression force, rotation speed, dissolution medium, and surfactant (SLS) concentration were determined during the development

of the intrinsic dissolution method. Drug powder was compressed at pressures ranging from 100 to 2000 psi for 1 and 30 min. Rotation speeds of 50, 100, 150, and 200 rpm were evaluated. The dissolution media used were 0.1 N hydrochloric acid pH 1.2, 0.05 M acetate buffer pH 4.5, water pH 5.5, and 0.05 M sodium phosphate buffer pH 6.8. SLS was used in these media at concentrations of 0.5, 1.0, and 2.0% (w/v). The dissolution media were prepared according to *USP* specifications (*19*).

The compact disks of efavirenz were evaluated considering the disk surface aspects and hardness and were characterized by XDR. XDR analysis was performed as described above as recommended by the *USP* to determine if the applied compression force changed the crystalline structure of the drug (*19*). Compact disks of each batch were evaluated and removed from the rotating disk holder at the completion of the dissolution test. The final dissolution conditions that were selected were also analyzed by XDR to investigate whether any polymorphic changes occurred during dissolution (*19*).

Intrinsic Dissolution Rate of Different Efavirenz Raw Materials

The different batches of efavirenz (A–G) were analyzed by the intrinsic dissolution method that was developed. The IDR was determined from the slope of the intrinsic dissolution–time profiles and was expressed in µg/min/cm^2. All experiments were performed in triplicate.

Statistical Analysis

Statistical analysis of the dissolution data was performed using one-way ANOVA and Tukey's multiple comparisons test with the aid of GraphPadprisma software (Version 5.0, GraphPad Software, Inc., 2007).

RESULTS AND DISCUSSION

Drug Characterization

The XRD technique indicates that the crystalline state of the efavirenz batches (Figure 1) was present as Form I since the characteristic signals were observed at 12.9°, 20.3°, 22.65°, and 29.6°. Form I is the most stable polymorph of efavirenz and is commonly used in pharmaceutical formulations (*35*, *36*). The DSC thermogram (Figure 2) shows that the endothermic melting curves of efavirenz batches were between 138 and 141 °C. The mean onset and endset temperatures were around 138.7 °C and 140.5 °C, respectively (ΔH = 44.6 J/g). Additional peaks indicative of polymorphic transitions were not observed and confirmed results obtained from XRD, indicating that the evaluated samples contained only polymorph I (*35*, *36*).

Efavirenz batches A–G presented different distributions of particle size and specific surface area values, as shown in Table 1. Batches A, D, and G presented mean particle sizes ranging from 2.0 to 2.38 µm, batches C and F presented mean values around 3.5 µm, while batches B and E showed the largest particle sizes at 5.779 and 4.980 µm, respectively. The modal values of the particle size distributions were superior to the respective mean and median values for all batches of efavirenz, especially for batches B and E. This parameter indicates the most frequent particle size in the batch, and in some cases, it is the most representative parameter for evaluation of particle size distribution (*37*). The modal value of the particle size distribution was notable for batch B (21.825 µm) indicating that this batch possessed the largest particle size of the seven efavirenz batches evaluated. Large PI values were found in batches C and G, present especially in batch G, demonstrating that the diameter of the particles was not homogeneous in these batches. The specific surface area ranged between 2.0 and 9.0 m^2/g, with emphasis on batch A, which showed a greater surface area than the other batches, 8.6790 m^2/g, compared with batch B, which

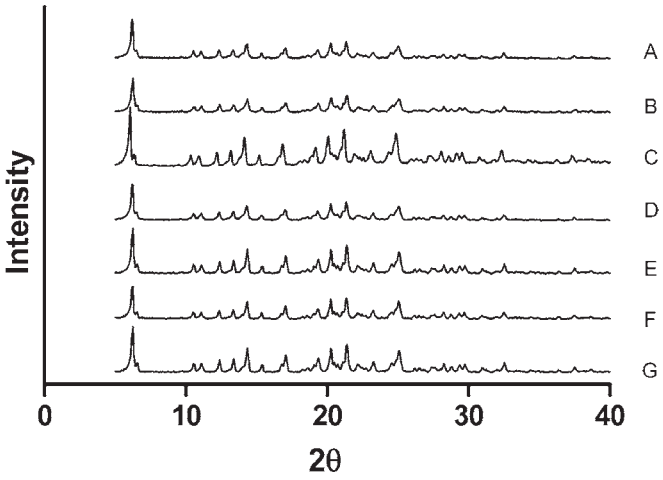

Figure 1. X-ray diffractograms of efavirenz batches A–G.

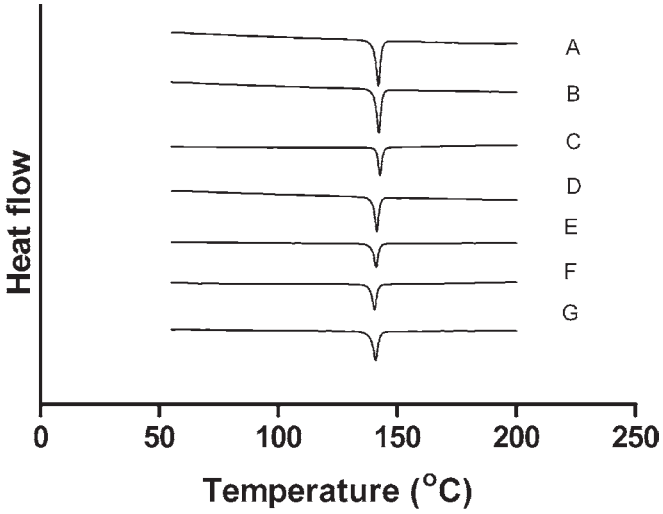

Figure 2. DSC thermograms of efavirenz batches A–G.

Table 1. Particle Size Distribution and Surface Area of Efavirenz Batches

Batch	Surface Area (m^2/g)	Particle Size Distribution (µm)			
		Mean	Median	Mode	Polydispersion index
A	8.679	2.213	3.288	4.860	2.752
B	2.003	5.779	17.077	21.825	2.724
C	3.894	3.341	6.166	15.377	4.430
D	6.257	2.037	2.736	5.558	2.441
E	2.739	4.980	11.656	15.657	2.751
F	5.230	3.833	7.699	13.484	3.038
G	5.067	2.378	3.443	8.336	6.414

showed the lowest value, 2.0030 m^2/g. The surface area values were consistent with the respective values obtained for particle size.

Figure 3 presents the morphology of the efavirenz batches analyzed by SEM. Batches A and D showed rod-shaped crystals that were comparatively smaller and shorter than the other batches of efavirenz analyzed, which is in agreement with the obtained values of particle size and surface area (Table 1). The particle size in batches B and E was visually larger than in other batches with a marked 7500× increase. Examination of the morphological aspects of batch B revealed that it was predominantly made up of clusters of long rod-shaped crystals, which justifies the high mean particle diameter values and low surface area measurements of 5.779 µm and 2.0030 m^2/g, respectively.

Solubility

Table 2 shows the solubility of efavirenz in the different media evaluated, pH 1.2 hydrochloric acid, pH 4.5 acetate buffer, water pH 5.5, and pH 6.8 sodium phosphate buffer. In the absence of SLS surfactant, the highest solubility value observed was 12.3 µg/mL in pH 1.2 hydrochloric acid, while in other media without surfactant, the solubility values were closer to 10 µg/mL, as described in the literature for efavirenz (*4*, *38*). An increase in drug solubility was observed with an increase in surfactant concentration in the four media evaluated, and the highest solubility observed was 5.37 mg/mL in pH 6.8 sodium phosphate buffer with 2.0% SLS. The solubility of efavirenz in water, even in the presence of SLS, was lower than that observed in other media, confirming its poor water solubility and its behavior as a brick dust drug (*39*, *40*).

Table 2. Solubility of Efavirenz (mg/mL) in Different Media and SLS Concentrations

Medium	SLS concentration (% m/v)			
	0	0.5	1.0	2.0
Hydrochloric acid pH 1.2	0.0123	0.8889	2.0709	4.3188
Acetate buffer pH 4.5	0.0108	1.0168	2.3052	4.8428
Water pH 5.5	0.0093	1.0708	1.8663	2.9780
Phosphate buffer pH 6.8	0.0072	1.1446	2.5395	5.3727

Intrinsic Dissolution Method Development

Evaluation of Compression Force Parameter on IDR

The efavirenz compacts used for intrinsic dissolution testing were prepared using reduced levels of compression force and compression time that were still capable of generating a nondisintegrating compact material as specified by *USP* (*19*). Efavirenz has electrostatic behavior and stuck to the lower surface plate of the apparatus used for drug compression, resulting in fragmentation of the compacts when the plate was removed from the disk, as Yu et al. (*23*) reported for the drug metoprolol. The compacts prepared under compression forces up to 300 psi for 1 min and 600 psi for 30 s were slightly brittle, and drug was deposited on the base of the intrinsic dissolution apparatus. Under compression forces of 1500 and 2000 psi, the compacts appeared clearer and slightly opaque. To reduce the deposition of efavirenz and facilitate the preparation of compacts, a small amount of magnesium stearate was used to lubricate the base of the intrinsic dissolution apparatus, as described by Sehic et al. (*28*). With the lubricant, it was possible to obtain nondisintegrating compacts produced in the range of 300–1200 psi using both 1-min and 30-s compression times.

The XRD analyses of the compacts showed no changes in the crystalline structure of the drug after application of the compressive force, since the XRD patterns obtained with 30 s and 1 min of compression corresponded to the crystalline form I patterns of efavirenz and to the diffractograms (Figure 1) obtained before the application of compressive force (*35*, *36*). The compacts increased in hardness when prepared in the range of 100–1000 psi for 30 s, which indicates that the compacts became harder when subjected to increasing compression forces of up to 300 psi. The compact hardness obtained under a compression force of 100 psi was 17 N, and 24 N under a compression force of 300 psi. The hardness of the compacts

obtained under compression forces of 400–1000 psi was maintained in the range of 29–33 N. Compressive forces above 1000 psi were not evaluated due to the difficulty in removing the intact compact from the intrinsic dissolution apparatus for evaluation.

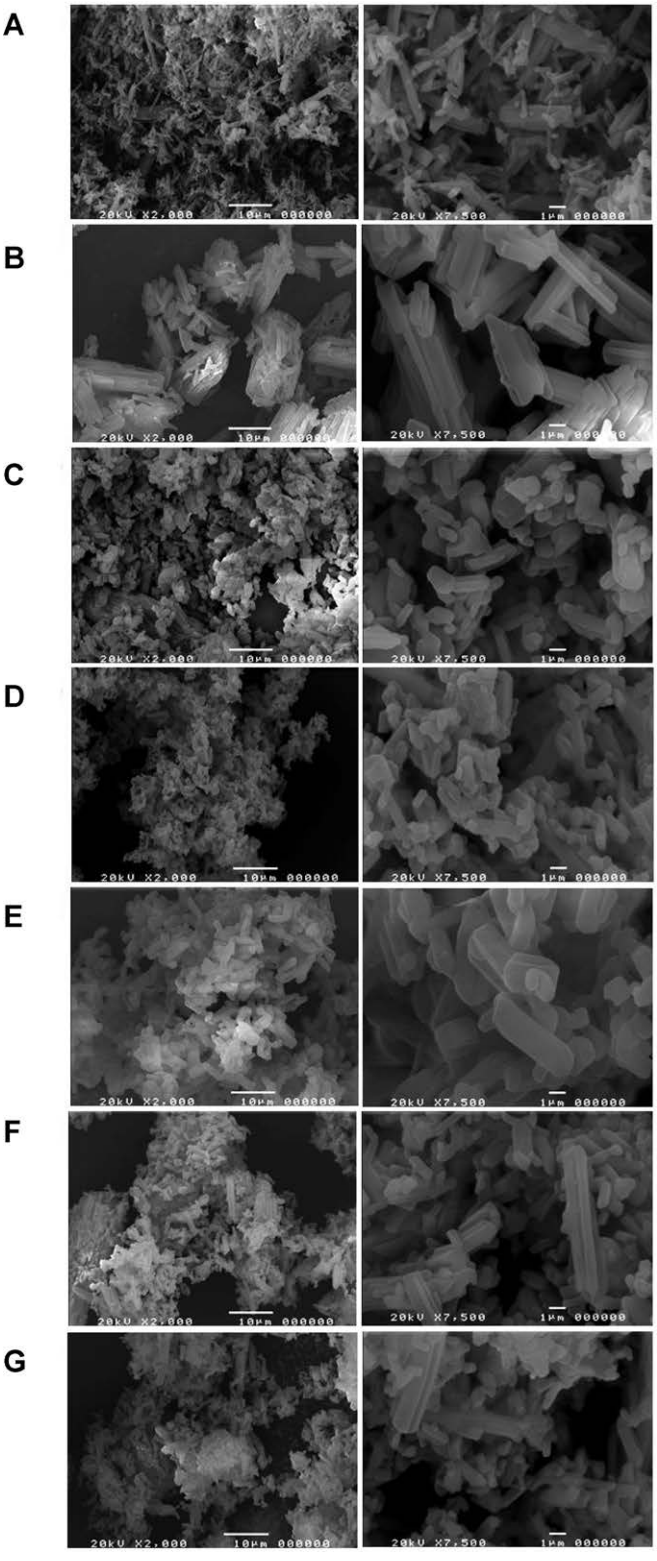

Figure 3. Scanning electron microscopy of efavirenz batches A–G.

Figure 4 shows the intrinsic dissolution profiles of efavirenz using compression forces of 100–1200 psi for 30 s, carried out in 500 mL of aqueous 0.5% SLS with a rotation speed of 50 rpm. After 5 h of dissolution testing, about 9 mg of drug dissolved from the compact at all the compression forces evaluated. This represents around 2.5% of the total mass used in the preparation of the compacts; this small percentage of dissolved drug is due to the low solubility of efavirenz in water and its behavior as a brick dust drug (*4*, *5*, *39*, *40*). The efavirenz IDR obtained from the compressive force ranging from 100–1200 psi was maintained between 26.33 and 28.99 µg/min/cm^2, and although the forces of 100, 150, and 300 psi provided a comparatively larger released mass by area, there was no statistically significant difference among the compression forces evaluated ($p > 0.05$).

The compression force is a parameter evaluated for the intrinsic dissolution test that can be crucial for some drugs, such as acetaminophen, which has its crystal habit destroyed during the compression process used to obtain the compact disk (*41*). The compression forces applied during this study do not alter the efavirenz IDR in the ranges tested. Accordingly, the intermediate compression force of 600 psi for 30 s was selected for the intrinsic dissolution method of efavirenz. Furthermore, using this compression force resulted in observable reproducibility of compact material preparation and resulted in a nondisintegrating compact. Compression forces similar to that adopted in this study were used to make rifampicin compacts (*26*). In that study, after evaluating compression forces between 100 and 5000 psi for 1 min and considering the possible polymorphic transitions, the authors used a pressure of 500 psi for 1 min as the ideal condition to obtain nondisintegrating compact material.

Evaluation of Rotation Speed Parameter on IDR

The effect of rotation speed on efavirenz IDR is shown in Figure 5, which also considers three different compression

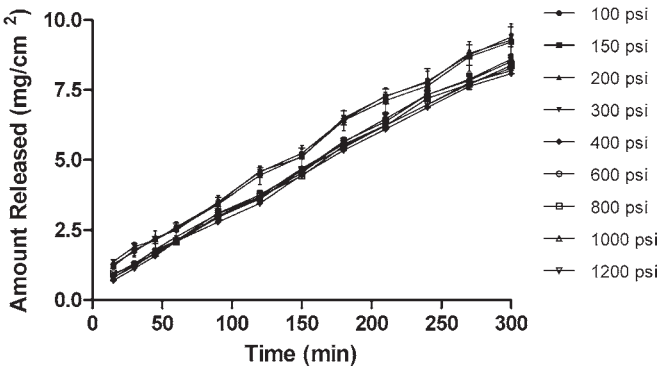

Figure 4. Comparative intrinsic dissolution profiles at different disk compression forces.

forces. The mean values of IDR measured at the rotation speeds 50, 100, 150, and 200 rpm were 27.24, 38.06, 61.66, and 58.82 µg/min/cm^2, respectively. The efavirenz IDR increased with increasing rotation speed up to 150 rpm. The amount of dissolved drug and the intrinsic dissolution profiles obtained from rotation speeds of 150 and 200 rpm were considered statistically similar ($p > 0.05$). In addition, there were also no statistical differences among the compressive forces of 200, 600, and 1000 psi evaluated at the same rotation speed ($p > 0.05$).

The *USP* recommends rotation speeds between 50 and 500 rpm (*19*). Intrinsic dissolution studies described in the literature (*23*, *26*, *28*, *42*, *43*) demonstrate that lower rotation speeds (i.e., 50 or 100 rpm) are ideal for use in discriminating methods. In this work, the rotation speed of 100 rpm was selected for the intrinsic dissolution of efavirenz to use milder, and therefore more discriminative, dissolution conditions (*44*).

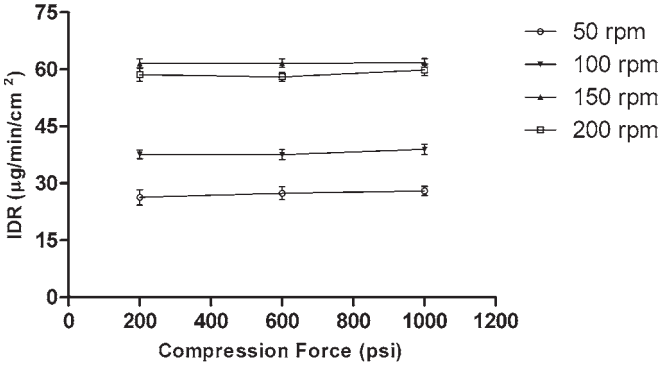

Figure 5. Intrinsic dissolution rates at different disk compression forces and rotation speeds.

Evaluation of Dissolution Medium Parameter on IDR

The dissolution media pH 1.2 hydrochloric acid, pH 4.5 acetate buffer, water pH 5.5, and pH 6.8 sodium phosphate buffer were tested without surfactant and with the addition of 0.5, 1.0, and 2.0% SLS. Table 3 shows that both the dissolved mass of drug at the end of the dissolution test and the IDR increased with increasing surfactant concentration in the four media assessed. The lowest IDR was observed in pH 1.2 hydrochloric acid. There were no significant differences among the dissolution rates in acetate buffer, water, and phosphate buffer media at the same SLS concentrations ($p > 0.05$). The correlation coefficient calculated from the intrinsic dissolution-versus-time profiles shows a high correlation ($r > 0.99$) indicating zero-order dissolution kinetics for all the conditions tested.

The media were selected to cover biorelevant conditions within the physiological pH range (1.2–6.8) to reflect the in vivo performance of the dosage form (*44*, *45*). However, water was selected as the dissolution medium due to the similarity in mass dissolved at the end of the dissolution test and the IDR between this medium and the other media tested, except for pH 1.2 hydrochloric acid. Moreover, this medium is consistent with the official monographs of pharmaceutical forms of efavirenz that adopt water containing surfactant SLS (*19*, *30–32*). Thus, the conditions of the dissolution test were 900 mL of water containing SLS as the dissolution medium with a rotation speed of 100 rpm.

Intrinsic Dissolution Rate of Different Efavirenz Raw Materials

Batches A and B were used to select a discriminative intrinsic dissolution method that can discern differences in bioavailability. In Figure 6, the intrinsic dissolution profiles in the various SLS concentrations demonstrate

Table 3. Intrinsic Dissolution Rate of Efavirenz in Different Dissolution Media

Dissolution Medium	SLS concentration (% m/v)	Mass dissolved (mg) in 5 h	IDR (µg/min/cm^2)
Hydrochloric acid pH 1.2	0.5	11.31	28.76 ± 0.97
	1.0	21.15	56.92 ± 1.04
	2.0	35.77	110.37 ± 4.68
Acetate buffer pH 4.5	0.5	12.09	35.23 ± 0.59
	1.0	20.57	63.09 ± 0.52
	2.0	41.98	142.32 ± 1.29
Water pH 5.5	0.5	11.53	36.87 ± 0.67
	1.0	21.21	68.34 ± 1.44
	2.0	38.64	114.32 ± 1.29
Phosphate buffer pH 6.8	0.5	12.48	36.08 ± 0.47
	1.0	21.79	67.56 ± 0.58
	2.0	40.63	126.85 ± 3.35

Medium: 900 mL; disk rotation speed 100 rpm; disk compression force 600 psi for 30 s. Mean ± SD; n = 3.

that increasing the concentration of surfactant, besides increasing the mass of drug dissolved, leads to more similar intrinsic dissolution profiles among these batches. Batches A and B were considered statistically different only in media containing 0.5% ($p < 0.001$) and 1.0% SLS ($p < 0.001$) according to ANOVA analysis. Evaluation of both intrinsic dissolution profiles in comparison to the IDR values (Table 4) shows differences between batches A and B at these surfactant concentrations, especially 0.5% SLS, indicating that the higher surfactant concentrations resulted in non-discriminatory media, as shown in other studies (*46–48*).

The reduction in the discriminatory capacity of the dissolution media upon increased surfactant concentrations was also verified in the other batches of efavirenz assessed, as can be seen in Table 4, which presents the IDR of batches A–G in water containing 0.5, 1.0, and 2.0% SLS. The dissolution medium containing 0.5% SLS was the most suitable for a comparative analysis between the batches and one-way analysis of variance ANOVA. A 0.5% concentration of surfactant allowed raw materials to be classified into groups. Batches A, D, and F were statistically equal ($p > 0.05$) and different from batches B and E ($p < 0.001$). Batches A, D, and F were classified as batches that release a higher mass of drug from the compact thus presenting higher IDR values (Group 1), while batches B and E were classified as batches with lower mass of released drug from the compact, with lower values of IDR (Group 2).

The IDR values observed using 0.5% SLS were consistent with the physicochemical characteristics of particle size and surface area of the batches assessed, since batches from Group 1 have smaller particle size and larger surface area, while the lots from Group 2 have larger particle size and smaller surface area. The interpretation of the IDR value cannot be performed in isolation; that is, for a comparison among different batches, it is necessary to critically evaluate the physicochemical characteristics in combination, considering all the parameters presented in Table 1. Consideration of the mean particle size in isolation does not always indicate the real characteristics of a batch, although it is necessary to assess the mode, $D_{0.1}$ and $D_{0.9}$ values, and the polydispersity indices (*37*). The IDR of the Group 1 and 2 batches were plotted versus the surface area and particle size parameters as shown in Table 1. The highest correlation coefficient value was 0.9181 obtained with the surface area data followed by the median and mean, $r = 0.8145$ and 0.8048, respectively.

The analysis of the dissolution residue found in batches A–G by XRD at the final intrinsic dissolution conditions containing 0.5% SLS indicates that there were no polymorphic changes to efavirenz after 5 h of analysis. XRD patterns similar to those shown in Figure 1 were obtained for these residues, confirming the presence of only polymorph I (data not shown).

The intrinsic dissolution method developed in this work can be applied in the development of efavirenz formulations to select the raw materials for use in the production

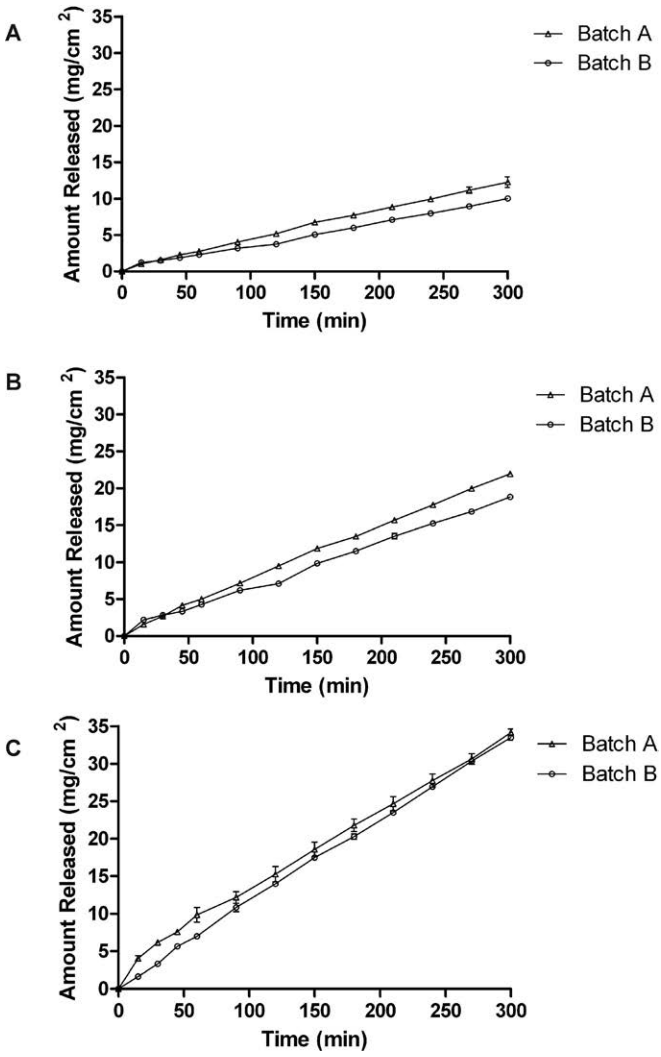

Figure 6. Comparative intrinsic dissolution profiles of efavirenz batches A and B at (A) 0.5%, (B) 1.0%, and (C) 2.0% concentrations of sodium lauryl sulfate (SLS) in the dissolution media. Dissolution conditions were compression force 600 psi for 30 s and100 rpm.

Table 4. Intrinsic Dissolution Rate (µg/min/cm²) of Different Lots of Efavirenz

Batch	SLS concentration (% m/v)		
	0.5	1.0	2.0
A	39.13 ± 1.60	71.08 ± 0.69	103.45 ± 3.41
B	31.26 ± 1.77	59.53 ± 0.79	110.95 ± 1.20
C	33.57 ± 0.30	65.64 ± 0.63	106.30 ± 0.26
D	36.87 ± 1.77	68.55 ± 2.00	114.39 ± 2.00
E	31.92 ± 1.15	63.09 ± 0.21	102.76 ± 2.41
F	37.33 ± 2.16	68.30 ± 0.93	106.97 ± 1.05
G	30.87 ± 2.34	67.63 ± 1.38	115.24 ± 1.31

Medium: 900 mL; disk rotation speed 100 rpm; disk compression force 600 psi for 30 s. Mean ± SD; n = 3.

of dosage forms that provide adequate bioavailability and dissolution. The tablets prepared using efavirenz API batch A were bioequivalent to the reference drug product, while the tablets prepared using batch B were not bioequivalent (*33*). Although both tablet batches (biobatches A and B) presented the same T_{max} (4.5 h), the pharmacokinetic parameters obtained for biobatch B (C_{max} = 1.09 ± 0.44 µg/mL; *AUC* = 65.10 ± 16.45 µg·h/mL) were about 50% less than those obtained for biobatch A (C_{max} = 2.93 ± 0.83 µg/mL; *AUC* = 137.95 ± 42.85 µg·h/mL) (*33*), showing that the properties of particle size and surface area influence drug absorption. The IDR values obtained from the evaluation of the seven batches of efavirenz and the bioequivalence test results for batches A and B suggest that a minimum IDR value of 35 µg/min/cm^2, using the intrinsic dissolution conditions described in this study, is an ideal specification of efavirenz API with the possibility of approval for the bioequivalence test. Tablets produced using batches D and F may provide adequate bioavailability, since these batches showed similar performance to that observed in batch A approved in the bioequivalence test. Similarly, tablets produced using batch E may not provide adequate bioavailability.

CONCLUSIONS

In this study, an intrinsic dissolution method was developed that was applicable for quality control of efavirenz raw material using the USP rotating disk method (Wood's apparatus). The compression force had no effect on the IDR of the drug, and IDR values were higher with increasing rotation speeds up to 150 rpm. The method for preparation of the compacts did not change the crystal structure of efavirenz, as shown by XRD analyses. Water containing 0.5% SLS was the most discriminative dissolution medium for the comparative evaluation of different efavirenz batches based on their particle size distributions and surface area properties. The method developed for intrinsic dissolution resulted in a high correlation between surface area of the API batch and its IDR value.

ACKNOWLEDGMENTS

The authors wish to thank CAPES, CPNq, and FAPERJ for the financial support. We are grateful to Michelle Parvatiyar for her English review.

REFERENCES

1. Maggiolo, F. Efavirenz: a decade of clinical experience in the treatment of HIV. *J. Antimicrob. Chemother.* **2009**, *64* (5), 910–928. DOI: 10.1093/jac/dkp334.
2. *Antiretroviral Therapy for HIV Infection in Adults and Adolescents: Recommendations for a public health approach*. World Health Organization: Geneva, 2010. http://whqlibdoc.who.int/publications/2010/9789241599764_eng.pdfua=1 (accessed April 15, 2014).
3. Thompson, M. A.; Aberg, J. A.; Hoy, J. F.; Telenti, A.; Benson, C.; Cahn, P.; Eron, J. J.; Günthard, H. F.; Hammer, S. M.; Reiss, P.; Richman, D. D.; Rizzardini, G.; Thomas, D. L.; Jacobsen, D. M.; Volberding, P. A. Antiretroviral treatment of adult HIV infection: 2012 recommendations of the International Antiviral Society–USA panel. *JAMA* **2012**, *308* (4), 387–402. DOI: 10.1001/jama.2012.7961.
4. Kasim, N. A.; Whitehouse, M.; Ramachandran, C.; Bermejo, M.; Lennerna, H.; Hussain, A. S.; Junginger, H. E.; Stavchansky, S. A.; Midha, K. K.; Shah, V. P.; Amidon, G. L. Molecular Properties of WHO Essential Drugs and Provisional Biopharmaceutical Classification. *Mol. Pharm.* **2004**, *1* (1), 85–96. DOI: 10.1021/mp034006h.
5. Lindenberg, M.; Kopp, S.; Dressman, J. B. Classification of orally administered drugs on the World Health Organization list of Essential Medicines according to the biopharmaceutics classification system. *Eur. J. Pharm. Biopharm*. **2004**, *58* (2), 265–278. DOI: 10.1016/j.ejpb.2004.03.001.
6. Rajesh, Y. V.; Balasubramaniam, J; Bindu, K.; Sridevi, R.; Swetha, M.; Rao, V. U. Impact of superdisintegrants on efavirenz release from tablet formulations. *Acta Pharm.* **2010**, *60* (2), 185–195. DOI: 10.2478/v10007-010-0019-6.
7. Sathigari, S.; Chadha, G.; Lee, Y. L.; Wright, N.; Parsons, D. L.; Rangari, V. K.; Fasina, R.; Babu, J. Physicochemical Characterization of Efavirenz–Cyclodextrin Inclusion Complexes. *AAPS PharmSciTech* **2009**, *10* (1), 81–87. DOI: 10.1208/s12249-008-9180-3.
8. Shown, I.; Banerjee, S.; Ramchandran, A. V.; Geckeler, K. E.; Murthy, C. N. Synthesis of Cyclodextrin and Sugar-Based Oligomers for Efavirenz Drug Delivery. *Macromol. Symp.* 2**010**, *287* (1), 51–59. DOI: 10.1002/masy.201050108.
9. Yang, J.; Grey, K.; Doney, J. An improved kinetics approach to describe the physical stability of amorphous solid dispersions. *Int. J. Pharm.* **2010**, *384* (1–2), 24–31. DOI: 10.1016/j.ijpharm.2009.09.035.
10. Madhavi, B. B.; Kusum, B.; Charanya, C. K.; Madhu, M. N.; Harsa, V. S.; Banji, D. Dissolution enhancement of efavirenz by solid dispersion and PEGylation techniques. *Int. J. Pharm. Invest.* **2011**, *1* (1), 29–34. DOI: 10.4103/2230-973X.76726.
11. Chiappetta, D. A.; Hocht, C.; Taira, C.; Sosnik, A. Efavirenz-loaded polymeric micelles for pediatric anti-HIV pharmacotherapy with significantly higher oral bioavailability. *Nanomedicine* **2010**, *5* (1), 11–23. DOI: 10.2217/nnm.09.90.
12. Chiappetta, D. A.; Hocht, C.; Taira, C.; Sosnik, A. Oral pharmacokinetics of the anti-HIV efavirenz encapsulated with polymeric micelles. *Biomaterials* **2011**, *32* (9), 2379–2387. DOI: 10.1016/j.biomaterials.2010.11.082.
13. Dressman, J. B.; Amidon, G. L.; Reppas, C.; Shah, V. P. Dissolution Testing as a Prognostic Tool for Oral Drug Absorption: Immediate Release Dosage Forms. *Pharm. Res*. **1998**, *15* (1), 11–22. DOI: 10.1023/A:1011984216775.

14. Dokoumetzidis, A.; Macheras, P. A century of dissolution research: From Noyes and Whitney to the Biopharmaceutics Classification System. *Int. J. Pharm.* **2006**, *321* (1–2), 1–11. DOI: 10.1016/j.ijpharm.2006.07.011.
15. Dickinson, P. A.; Lee, W. W.; Stott, P. W.; Townsend, A. I.; Smart, J. P.; Ghahramani, P.; Hammett, T.; Billett, L.; Behn, S.; Gibb, R.C.; Abrahamsson, B. Clinical Relevance of Dissolution Testing in Quality by Design. *AAPS J.* **2008**, *10* (2), 380–390. DOI: 10.1208/s12248-008-9034-7.
16. Kesisoglou, F.; Wu, Y. Understanding the Effect of API Properties on Bioavailability Through Absorption Modeling. *AAPS J.* **2008**, *10* (4), 516–525. DOI: 10.1208/s12248-008-9061-4.
17. Kawabata, Y.; Wada, K.; Nakatani, M.; Yamada, S.; Onoue, S. Formulation design for poorly water-soluble drugs based on biopharmaceutics classification system: Basic approaches and practical applications. *Int. J. Pharm.* **2011**, *420* (1), 1–10. DOI: 10.1016/j.ijpharm.2011.08.032.
18. Ayres, C.; Burke, W.; Dickinson, P.; Kirk, G.; Pugh, R.; Sharma–Singh, G.; Kittlety, R. Intrinsic dissolution rate determinations in early development and relevance to in vivo performance. *Am. Pharm. Rev.* **2007**, *10* (1), 74–78.
19. *The United States Pharmacopeia and National Formulary USP 34–NF 29*; The United States Pharmacopeial Convention, Inc.: Rockville, MD, 2011.
20. Shete, G.; Puri, V.; Kumar, L.; Bansal, A. K. Solid state characterization of commercial crystalline and amorphous atorvastatin calcium samples. *AAPS PharmSciTech* **2010**, *11* (2), 598–609. DOI: 10.1208/s12249-010-9419-7.
21. Tsutsumi, S.; Iida, M.; Tada, N.; Kojima, T.; Ikeda, Y.; Moriwaki, T.; Higashib, K.; Moribeb, K.; Yamamotob, K. Characterization and evaluation of miconazole salts and cocrystals for improved physicochemical properties. *Int. J. Pharm.* **2011**, *421* (2), 230–236. DOI: 10.1016/j.ijpharm.2011.09.034.
22. Gilchrist, S. E; Letchford, K.; Burt, H. M. The solid-state characterization of fusidic acid. *Int. J. Pharm.* **2012**, *422* (1–2), 245–253. DOI: 10.1016/j.ijpharm.2011.11.005.
23. Yu, L. X.; Carlin, A. S.; Amidon, G. L.; Hussain, A. S. Feasibility studies of utilizing disk intrinsic dissolution rate to classify drugs. *Int. J. Pharm.* **2004**, *270* (1–2), 221–227. DOI: 10.1016/j.ijpharm.2003.10.016.
24. Zakeri-Milani, P.; Barzegar-Jalali, M.; Azimi, M.; Valizadeh, H. Biopharmaceutical classification of drugs using intrinsic dissolution rate (IDR) and rat intestinal permeability. *Eur. J. Pharm. Biopharm.* **2009**, *73* (1), 102–106. DOI: 10.1016/j.ejpb.2009.04.015.
25. Issa, M. G.; Ferraz, H. G. Intrinsic Dissolution as a Tool for Evaluating Drug Solubility in Accordance with the Biopharmaceutics Classification System. *Dissolution Technol.* **2011**, *18* (3), 6–13.
26. Agrawal, S.; Ashokraj, Y.; Bharatam, P. V.; Pillai, O.; Panchagnula, R. Solid-state characterization of rifampicin samples and its biopharmaceutic relevance. *Eur. J. Pharm. Sci.* **2004**, *22* (2–3), 127–144. DOI: 10.1016/j.ejps.2004.02.011.
27. Carini, J. P.; Pavei, C.; Silva, A. P. C.; Machado, G.; Mexias, A. S.; Pereira, V. P.; Fialho, S. L.; Mayorga, P. Solid state evaluation of some thalidomide raw materials. *Int. J. Pharm.* **2009**, *372* (1–2), 17–23. DOI: 10.1016/j.ijpharm.2008.12.034.
28. Šehić, S.; Betz, G.; Hadžidedić, S.; El-Arini, S. K.; Leuenberguer, H. Investigation of intrinsic dissolution behavior of different carbamazepine samples. *Int. J. Pharm.* **2010**, *386* (1–2), 77–90. DOI: 10.1016/j.ijpharm.2009.10.051.
29. Flicker, F.; Eberle, V. A.; Betz, G. Variability in commercial carbamazepine samples—Impact on drug release. *Int. J. Pharm.* **2011**, *410* (1–2), 99–106. DOI: 10.1016/j.ijpharm.2011.03.032.
30. Dissolution Methods Database. U.S. Food and Drug Administration Web site. http://www.accessdata.fda.gov/scripts/cder/dissolution/dsp_SearchResults_Dissolutions.cfm?PrintAll=1 (accessed April 15, 2014).
31. *Brazilian Pharmacopoeia*, 5th ed.; Brazilian Health Surveillance Agency: Brasília, 2010.
32. *The International Pharmacopoeia*, 4th ed.; Dept. of Essential Medicines and Pharmaceutical Policies, World Health Organization: Geneva, 2011.
33. Honorio, T. S.; Pinto, E. C.; Rocha, H. V. A.; Esteves, V. S. D.; dos Santos, T. C.; Castro, H. C. R.; Rodrigues, C. R.; de Sousa, V. P.; Cabral, L. M. In Vitro–In Vivo Correlation of Efavirenz Tablets using Gastroplus®. *AAPS PharmSciTech* **2013**, *14* (3), 1244–1254. DOI: 10.1208/s12249-013-0016-4.
34. Wood, J. H.; Syarto, J. E.; Letterman, H. Improved holder for intrinsic dissolution rate studies. *J. Pharm. Sci.* **1965**, *54* (7), 1068. DOI: 10.1002/jps.2600540730.
35. Chadha, R.; Arora, P.; Saini, A.; Jain, D. S. An insight into thermodynamic relationship between polymorphic forms of efavirenz. *J. Pharm. Pharm. Sci*. **2012**, *15* (2), 234–251.
36. Mahapatra, S.; Thakur, T. S.; Joseph, S.; Varughese, S.; Desiraju, G. R. New Solid State Forms of the Anti-HIV Drug Efavirenz. Conformational Flexibility and High Z Issues. *Cryst. Growth Des.* **2010**, *10* (7), 3191–3202. DOI: 10.1021/cg100342k.
37. da Fonseca, L. B.; Labastie, M.; de Sousa, V. P.; Volpato, N. M. Development and Validation of a Discriminative Test for Nimesulide Suspensions. *AAPS PharmSciTech* **2009**, *10* (4), 1145–1152. DOI: 10.1208/s12249-009-9320-4.
38. Rabel, S. R.; Maurin, M. B.; Rowe, S. M.; Hussain, M. Determination of the pK_a and pH–Solubility Behavior of an Ionizable Cyclic Carbamate, (S)-6-Chloro-4-(cyclopropylethyny1)-1,4-dihydro-4-(trifluoromethyl)-2H-3,1-benzoxazin-2-one (DMP

266). *Pharm. Dev. Technol.* **1996**, *1* (1), 91–95. DOI: 10.3109/10837459609031422.
39. Bergström, C. A. S.; Wassvik, C. M.; Johansson, K.; Hubatsch, I. Poorly Soluble Marketed Drugs Display Solvation Limited Solubility. *J. Med. Chem.* **2007**, *50* (23), 5858–5862. DOI: 10.1021/jm0706416.
40. Stella, V. J.; Nti-Addae, K. W. Prodrug strategies to overcome poor water solubility. *Adv. Drug Delivery Rev.* **2007**, *59* (7), 677–694. DOI: 10.1016/j.addr.2007.05.013.
41. Chan, H.-K.; Grant, D. J. W. Influence of compaction on the intrinsic dissolution rate of modified acetaminophen and adipic acid crystals. *Int. J. Pharm.* **1989**, *57* (2), 117–124. DOI: 10.1016/0378-5173(89)90299-8.
42. Bartolomei, M.; Bertocchi, P.; Antoniella, E.; Rodomonte, A. Physico-chemical characterisation and intrinsic dissolution studies of a new hydrate form of diclofenac sodium: comparison with anhydrous form. *J. Pharm. Biomed. Anal.* **2006**, *40* (5), 1105–1113. DOI: 10.1016/j.jpba.2005.09.009.
43. Park, H. J.; Kim, M.-S.; Kim, J.-S.; Cho, W.; Park, J.; Cha, K.-H.; Kang, Y.-S.; Hwang, S.-J. Solid-State Carbon NMR Characterization and Investigation of Intrinsic Dissolution Behavior of Fluconazole Polymorphs, Anhydrate Forms I and II. *Chem. Pharm. Bull.* **2010**, *58* (9), 1243–1247. DOI: 10.1248/cpb.58.1243.
44. Brown, C. K.; Chokshi, H. P.; Nickerson, B.; Reed, R. A.; Rohrs, B. R.; Shah, P. S. Acceptable analytical practices for dissolution testing of poorly soluble compounds. *Pharm. Technol.* **2004**, *28* (12), 56–65.
45. Qureshi, S. Developing Discriminatory Drug Dissolution Tests and Profiles: Some Thoughts for Consideration on the Concept and Its Interpretation. *Dissolution Technol.* **2006**, *13* (4), 18–23.
46. Pabla, D.; Akhlaghi, F.; Zia, H. A comparative pH-dissolution profile study of selected commercial levothyroxine products using inductively couple plasma mass spectrometry. *Eur. J. Pharm. Biopharm.* **2009**, *72* (1), 105–110. DOI: 10.1016/j.ejpb.2008.10.008.
47. Rossi, R. C.; Dias, C. L.; Bajerski, L.; Bergold, A. M.; Fröehlich, P. E. Development and validation of discriminating method of dissolution for fosamprenavir tablets based on in vivo data. *J. Pharm. Biomed. Anal.* **2011**, *54* (3), 439–444. DOI: 10.1016/j.jpba.2010.09.004.
48. Jamzad, S.; Fassihi, R. Role of surfactant and pH on dissolution properties of fenofibrate and glipizide—A technical note. *AAPS PharmSciTech* **2006**, *7* (2), E17–E22. DOI: 10.1208/pt070233.